EDN: MGVVRP
УДК 539.3

Physically Nonlinear Deformation of the Shell Using a Three-field FEM

Mikhail Yu. Klochkov*
Volgograd State Technical University
Volgograd, Russian Federation
Anatoly P. Nikolaev†
Volgograd State Agricultural University
Volgograd, Russian Federation
Valeria A. Pshenichkina‡
Volgograd State Technical University
Volgograd, Russian Federation
Olga V. Vakhnina§
Aleksandr S. Andreev¶
Yuri V. Klochkov‖
Volgograd State Agricultural University
Volgograd, Russian Federation

Received 10.08.2024, received in revised form 15.09.2024, accepted 24.10.2024

Abstract. A method has been developed for implementing an algorithm for determining the stress-strain state (SSS) of a thin shell based on the finite element method (FEM) in a three-field formulation under step loading. A quadrangular fragment of the median surface of the thin shell is accepted as the finite element. Nodal unknowns at the loading step used: increments of kinematic quantities (increments of displacements and their derivatives); increments of deformation quantities (increments of deformations and curvatures of the median surface); increments of force values (increments of forces and moments). The approximation of kinematic quantities was carried out using bicubic shape functions based on Hermite polynomials of the third degree, and force and deformation quantities using bilinear functions. To account for the physical nonlinearity of the shell material, the defining equations are used in two versions: the first is the defining equations of the theory of plastic flow and the second is the defining equations based on the proposed hypothesis of proportionality a component of deviators of strain increments and stress increments. The stiffness matrix of the finite element is formed on the basis of a nonlinear Lagrange functional for the loading step, expressing the equality of possible and actual work of given loads and internal forces, with the complementary condition that the actual work of the increments of internal forces is equal to zero on the difference in increments of deformation quantities determined by geometric relations and using approximating expressions. An example of calculation is given using the resulting finite element stiffness matrix.

Keywords: finite element in the three-field formulation, physical nonlinearity of the material, variants of the governing equations, nonlinear Lagrange functional with condition.

*m.klo4koff@yandex.ru https://orcid.org/0000-0001-6751-4629
†anpetr40@yandex.ru https://orcid.org/0000-0002-7098-5998
‡vap_hm@list.ru https://orcid.org/0000-0001-9148-2815
§ovahnina@bk.ru https://orcid.org/0000-0001-9243-7287
¶aandreev.07.1988@gmail.com https://orcid.org/0000-0002-3763-0394
‖klotchkov@bk.ru https://orcid.org/0000-0002-1027-1811

Citation: Yu.V. Klochkov, A.P. Nikolaev, V.A. Pshenichkina, O.V. Vakhnina, A.S. Andreev, M.Yu. Klochkov, Physically Nonlinear Deformation of the Shell Using a Three-field FEM, J. Sib. Fed. Univ. Math. Phys., 2025, 18(2), 207–215. EDN: MGVVRP.

Shell structures are widely used in various areas of engineering — in shipbuilding, aircraft manufacturing, in the creation of chemical engineering objects, in the aerospace industry and in many other branches of engineering. Nonlinear behavior of the material occurs in many areas of the considered thin-walled elements of engineering structures. To determine the stress-strain state in such areas, numerical calculation methods are usually used, among which the most widely used is the FEM in the formulation of the displacement method, when displacements and their derivatives of different orders are taken as nodal unknowns. A disadvantage of the FEM in the displacement method version is the lack of compatibility in terms of deformations at the boundaries between adjacent elements. To overcome this drawback, the FEM began to be used in a mixed version, where kinematic unknowns (displacements and their derivatives) and force unknowns (forces and moments) are used as nodal unknowns, where, when using bilinear approximation, convergence in force parameters at the boundaries of adjacent finite elements was ensured [1, 2].

The finite element method in a mixed version is used in studies of the stability of nonlinearly deformed elastic structures [3–5], as well as in determining the stress-strain state of structures taking into account the physical nonlinearity of the material [6–12]. In elastic-plastic deformation, the total strains are determined by differentiating the strain energy function with respect to stresses. Plastic strain is determined by the difference between the total and elastic strains. Displacements and stresses are taken as unknown quantities. When using the three-field FEM version [13], plastic multipliers are added to the nodal unknowns.

In this paper, a finite element in the form of a quadrangular fragment of the middle surface of a thin shell with three fields of nodal unknowns: kinematic, deformation and force is developed. In the first variant, the equations of the theory of plastic flow are used as the governing equations at the loading step. In the second variant, the governing equations at the loading step are obtained without separating the strain increments into elastic and plastic parts, based on the hypothesis of proportionality of the components of the deviators of strain increments and stress increments. To obtain the stiffness matrix of the finite element at the loading step, a nonlinear Lagrange functional is used with the condition of zero work of the increments of internal forces on the difference in the strain increments determined by geometric relations and found using approximating expressions directly.

1. Geometrical relationships of a thin shell

The position of an arbitrary point M^0 of the mid-surface of the shell is determined by the radius vector

$$\vec{R}^0 = x^m(\theta^\alpha)\vec{i}_m, \tag{1.1}$$

where x^m, $\vec{i}_m$ are the coordinates and orthants of the Cartesian coordinate system; θ^α are the curvilinear coordinates of the point.

The basis vectors of the point M^0 are defined by the expressions

$$\vec{a}^0_\alpha = \vec{R}^0_{,\alpha};\ \vec{a}^0_3 = \frac{\vec{a}^0_1 \times \vec{a}^0_2}{|\vec{a}^0_1 \times \vec{a}^0_2|} = \frac{\vec{a}^0_1 \times \vec{a}^0_2}{\sqrt{a^0}}. \tag{1.2}$$

The derivatives (1.2) are written as components in the same basis

$$\underset{3\times1}{\{\vec{a}^0_{,1}\}} = \underset{3\times3}{[m]}\underset{3\times1}{\{\vec{a}^0\}};\quad \underset{3\times1}{\{\vec{a}^0_{,2}\}} = \underset{3\times3}{[n]}\underset{3\times1}{\{\vec{a}^0\}}, \tag{1.3}$$

where $\underset{1\times3}{\{\vec{a}^0_{,\alpha}\}^T} = \{\vec{a}^0_{1,\alpha}\ \vec{a}^0_{2,\alpha}\ \vec{a}^0_{3,\alpha}\}$; $\underset{1\times3}{\{\vec{a}^0\}^T} = \{\vec{a}^0_1\ \vec{a}^0_2\ \vec{a}^0_3\}$.

The displacement vector of the point M^0 and its derivatives are defined in the basis of the same point

$$\vec{v} = v^\rho\vec{a}^0_\rho + v\vec{a}^0_3;\quad \vec{v}_{,\alpha} = f^\rho_\alpha\vec{a}^0_\rho + f_\alpha\vec{a}^0_3;\quad \vec{v}_{,\alpha\beta} = f^\rho_{\alpha\beta}\vec{a}^0_\rho + f_{\alpha\beta}\vec{a}^0_3, \tag{1.4}$$

where the components $f^\rho_\alpha,\ f_\alpha,\ f^\rho_{\alpha\beta},\ f_{\alpha\beta}$ are defined using (1.3).

Deformations and curvatures of the median surface at the point M^0 are determined by the relations [14]

$$\Delta\varepsilon_{\alpha\beta} = \frac{1}{2}(\vec{a}^0_\alpha\cdot\vec{v}_{,\beta}+\vec{a}^0_\beta\cdot\vec{v}_{,\alpha});\ \Delta\varkappa_{\alpha\beta} = \frac{1}{2}[\vec{a}^0_\alpha(\vec{a}_{3,\beta}-\vec{a}^0_{3,\beta})+\vec{a}^0_\beta(\vec{a}_{3,\alpha}-\vec{a}^0_{3,\alpha})+\vec{a}^0_{3,\alpha}\cdot\vec{v}_{,\beta}+\vec{a}^0_{3,\beta}\cdot\vec{v}_{,\alpha}]. \tag{1.5}$$

where $\vec{a}_{3,\alpha} = \dfrac{1}{\sqrt{a^0}}(\vec{a}_{1,\alpha}\times\vec{a}_2 + \vec{a}_1\times\vec{a}_{2,\alpha})$; $\vec{a}_\alpha = \vec{a}^0_\alpha + \vec{v}_{,\alpha}$; $\vec{a}_{\alpha,\rho} = \vec{a}^0_{\alpha,\rho} + \vec{v}_{,\alpha\rho}$.

On the basis of (1.5) we can form a matrix relation

$$\underset{6\times1}{\{\Delta\varepsilon\}} = \underset{6\times3}{[L]}\underset{3\times1}{\{\Delta U\}}, \tag{1.6}$$

where $\underset{1\times6}{\{\Delta\varepsilon\}^T} = \{\Delta\varepsilon_{11}\ \Delta\varepsilon_{22}\ 2\Delta\varepsilon_{12}\ \Delta\varkappa_{11}\ \Delta\varkappa_{22}\ 2\Delta\varkappa_{12}\}$; $\underset{1\times3}{\{\Delta U\}^T} = \{\Delta v^1\Delta v^2\Delta v\}$.

2. Defining equations

In the first variant, the equations of plastic flow theory were used, according to which the incremental strains at an arbitrary point of the shell are composed of elastic and plastic strains

$$\Delta\varepsilon^\zeta_{\alpha\beta} = \Delta\varepsilon^{\zeta e}_{\alpha\beta} + \Delta\varepsilon^{\zeta P}_{\alpha\beta}. \tag{2.1}$$

The elastic strain increments are determined by the relations [15]

$$\Delta\varepsilon^{e\zeta}_{\alpha\beta} = \frac{1}{2\mu}\Delta\sigma_{\alpha\beta} - g_{\alpha\beta}\lambda P_{\Delta\sigma}\frac{3}{2}\frac{1-2\nu}{2\mu}, \tag{2.2}$$

where $\lambda,\ \mu$ are the Lame parameters; ν is the transverse strain coefficient; $P_{\Delta\sigma} = \Delta\sigma_{\rho\tau}g^{\rho\tau}$ — first invariant of the stress increment tensor; $g_{\alpha\beta},\ g^{\alpha\beta}$ — components of the metric tensor.

Plastic strain increments in the flow theory are determined on the basis of the hypothesis of proportionality of plastic strain increments to the components of the stress deviator

$$\Delta\varepsilon^{\zeta P}_{\alpha\beta} = \frac{3}{2\sigma_i}\varphi(\sigma_{\alpha\beta} - \frac{1}{3}g_{\alpha\beta}P_\sigma)\Delta\sigma_i, \tag{2.3}$$

where $\varphi = \dfrac{1}{E_k} - \dfrac{1}{E_1}$; E_1 is the modulus of the initial section of the strain diagram; E_k is the tangent modulus of the strain diagram; $\Delta\sigma_i = \dfrac{\partial\sigma_i}{\partial\sigma_{\rho\tau}}\Delta\sigma_{\rho\tau} = \underset{1\times3}{\{S\}^T}\underset{3\times1}{\{\Delta\sigma\}}$; σ_i — stress intensity; $\underset{1\times3}{\{\Delta\sigma\}^T} = \{\Delta\sigma_{11}\Delta\sigma_{22}\Delta\sigma_{12}\}$.

Based on (2.1), (2.2) and (2.3) a matrix relation is formed

$$\underset{3\times1}{\{\Delta\varepsilon^{\zeta}\}} = \underset{3\times3}{[C_1]}\underset{3\times1}{\{\Delta\sigma\}}. \tag{2.4}$$

In the second version of the defining relations, the hypothesis of separation of strain increments into elastic and plastic parts is not used. The defining equations are obtained on the basis of the hypothesis of proportionality of the components of the deviators of strain increments and stress increments

$$\Delta\varepsilon_{\alpha\beta} - \frac{1}{3}g_{\alpha\beta}P_{\Delta\varepsilon} = K(\Delta\sigma_{\alpha\beta} - \frac{1}{3}g_{\alpha\beta}P_{\Delta\sigma}), \tag{2.5}$$

where $K = \dfrac{3}{2E_{x\partial}}$; $P_{\Delta\varepsilon} = P_{\Delta\sigma}\dfrac{1-2\nu}{E}P_{\Delta\sigma}$; $P_{\Delta\sigma} = \Delta\sigma_{\rho\tau}g^{\rho\tau}$ is the first invariant of the stress increment tensor.

Based on (2.5) a matrix relation is formed

$$\underset{3\times1}{\{\Delta\varepsilon^{\zeta}\}} = \underset{3\times3}{[C_2]}\underset{3\times1}{\{\Delta\sigma\}}. \tag{2.6}$$

At an arbitrary point M^0 we introduce lines of increments of deformations and curvatures of the medial surface and lines of increments of internal forces and moments of the shell section, the relations between which are determined taking into account (2.4), (2.6) on the basis of the Kirchhoff–Lava hypothesis

$$\underset{6\times1}{\{\Delta S\}} = \underset{6\times6}{[h_\alpha]}\underset{6\times1}{\{\Delta\varepsilon\}}. \tag{2.7}$$

where

$$\underset{6\times1}{\{\Delta S\}^T} = \{\Delta N^{11}\ \Delta N^{22}\ \Delta N^{12}\ \Delta M^{11}\ \Delta M^{22}\ \Delta M^{12}\};$$
$$\{\Delta\varepsilon\} = \{\Delta\varepsilon_{11}\ \Delta\varepsilon_{22}\ 2\Delta\varepsilon_{12}\ \Delta\varkappa_{11}\ \Delta\varkappa_{22}\ 2\Delta\varkappa_{12}\}.$$

3. Stiffness matrix of the finite element

The finite element is taken in the form of a curvilinear quadrilateral fragment of the median surface with nodes i, j, k, l. The relations between kinematic, deformation and force parameters for the finite element are regulated at the loading step by a nonlinear variational Lagrangian functional with condition

$$\begin{gathered}\Pi_{LU} = \int\limits_F \left[\underset{1\times6}{\{S\}^T} + \frac{1}{2}\underset{1\times6}{\{\Delta S\}^T}\right]\underset{6\times1}{\{\Delta\varepsilon\}}dF - \int\limits_F \underset{1\times3}{\{\Delta U\}^T}\left[\underset{3\times1}{\{q\}} + \frac{1}{2}\underset{3\times1}{\{\Delta q\}}\right]dF + \\ +\frac{1}{2}\int\limits_F \underset{1\times6}{\{\Delta S\}^T}\left[\underset{6\times1}{\{\Delta\varepsilon^g\}} - \underset{6\times1}{\{\Delta\varepsilon^a\}}\right]dF,\end{gathered} \tag{3.1}$$

where the first expression means the possible and actual work of internal forces on the deformation values of the loading step. The second expression defines the possible and actual work of the given forces on the loading step. The third expression means the actual work of internal forces of the loading step on the difference of deformation values determined by geometrical formulae (through displacements) with subsequent approximation of displacements and deformation values found by their direct approximation.

The following kinematic nodal unknowns in the local $\{\Delta v_y^s\}$ and global $\{\Delta v_y^g\}$ coordinate systems are used for the finite element under consideration

$$\begin{gathered}\underset{1\times 36}{\{\Delta v_y^s\}^T}=\{\Delta v^{1i}\dots\Delta v^{1l}\Delta v^{1i}_{,\xi}\dots\Delta v^{1l}_{,\xi}\Delta v^{1i}_{,\eta}\dots\Delta v^{1l}_{,\eta}\Delta v^{2i}\dots\Delta v^{2l}\\ \Delta v^{2i}_{,\xi}\dots\Delta v^{2l}_{,\xi}\Delta v^{2i}_{,\eta}\dots\Delta v^{2l}_{,\eta}\Delta v^{i}\dots\Delta v^{l}\Delta v^{i}_{,\xi}\dots\Delta v^{l}_{,\xi}\Delta v^{i}_{,\eta}\dots\Delta v^{l}_{,\eta}\};\\ \underset{1\times 36}{\{\Delta v_y^g\}^T}=\{\Delta v^{1i}\dots\Delta v^{1l}\Delta v^{1i}_{,\alpha}\dots\Delta v^{1l}_{,\alpha}\Delta v^{1i}_{,\beta}\dots\Delta v^{1l}_{,\beta}\Delta v^{2i}\dots\Delta v^{2l}\\ \Delta v^{2i}_{,\alpha}\dots\Delta v^{2l}_{,\alpha}\Delta v^{2i}_{,\beta}\dots\Delta v^{2l}_{,\beta}\Delta v^{i}\dots\Delta v^{l}\Delta v^{i}_{,\alpha}\dots\Delta v^{l}_{,\alpha}\Delta v^{i}_{,\beta}\dots\Delta v^{l}_{,\beta}\},\end{gathered}\tag{3.2}$$

between which there is a matrix relation

$$\underset{36\times 1}{\{\Delta v_y^s\}}=\underset{36\times 36}{[T]}\,\underset{36\times 1}{\{\Delta v_y^g\}}.\tag{3.3}$$

The strain $\{\Delta E_y\}^T$ and force nodal unknowns $\{\Delta S_y\}^T$ were taken as follows lines

$$\begin{gathered}\underset{1\times 24}{\{\Delta E_y\}^T}=\{\underset{1\times 6}{\{\Delta E_y^i\}^T}\underset{1\times 6}{\{\Delta E_y^j\}^T}\underset{1\times 6}{\{\Delta E_y^k\}^T}\underset{1\times 6}{\{\Delta E_y^l\}^T}\};\\ \underset{1\times 24}{\{\Delta S_y\}^T}=\{\underset{1\times 6}{\{\Delta S_y^i\}^T}\underset{1\times 6}{\{\Delta S_y^j\}^T}\underset{1\times 6}{\{\Delta S_y^k\}^T}\underset{1\times 6}{\{\Delta S_y^l\}^T}\},\end{gathered}\tag{3.4}$$

where $\underset{1\times 6}{\{\Delta E_y^\lambda\}^T}=\{\Delta\varepsilon_{11}^\lambda\Delta\varepsilon_{22}^\lambda 2\Delta\varepsilon_{12}^\lambda\Delta\varkappa_{11}^\lambda\Delta\varkappa_{22}^\lambda 2\Delta\varkappa_{12}^\lambda\}$ — a string of strain and curvature increments at the nodal point; $\underset{1\times 6}{\{\Delta S_y^\lambda\}^T}=\{\Delta N^{11\lambda}\Delta N^{22\lambda}\Delta N^{12\lambda}\Delta M^{11\lambda}\Delta M^{22\lambda}\Delta M^{12\lambda}\}$ — line of force and moment increments at the nodal point λ; $\lambda=i,\ j,\ k,\ l$.

The approximation of the increments of displacements of the internal point of the finite element was carried out by the expression

$$\lambda=\underset{1\times 36}{\{\varphi(\xi,\eta)\}^T}\underset{36\times 1}{\{\Delta v_y^s\}},\tag{3.5}$$

where the symbol λ is Δv^1, Δv^2, Δv^2, Δv; the elements of the function $\{\varphi(\xi,\eta)\}$ are Hermite polynomials of degree three.

On the basis of (3.5) the matrix relations are formed

$$\underset{3\times 1}{\{\Delta U\}}=\underset{3\times 36}{[A]}\,\underset{36\times 1}{\{\Delta v_y^s\}};\quad \underset{6\times 1}{\{\Delta\varepsilon\}}=\underset{6\times 3}{[L]}\underset{3\times 1}{\{\Delta U\}}=\underset{6\times 3}{[L]}\,\underset{3\times 36}{[A]}\,\underset{36\times 1}{\{\Delta v_y^s\}}=\underset{6\times 36}{[B]}\,\underset{36\times 1}{\{\Delta v_y^s\}}.\tag{3.6}$$

Bilinear functions are used for approximation of deformations and forces on the basis of which matrix expressions are formed

$$\underset{6\times 1}{\{\Delta\varepsilon\}}=\underset{6\times 24}{[H]}\,\underset{24\times 1}{\{\Delta E_y\}};\quad \underset{6\times 1}{\{\Delta S\}}=\underset{6\times 24}{[H]}\,\underset{24\times 1}{\{\Delta S_y\}}.\tag{3.7}$$

Taking into account the approximating expressions (2.7), (3.3), (3.6), (3.7), the functional (3.1) is written by the expression

$$\begin{gathered}\Pi_{LU}=\underset{1\times 36}{\{\Delta U_y^g\}^T}\,\underset{36\times 36}{[T]}^T\int\limits_F\underset{36\times 6}{[B]}\,\underset{6\times 1}{\{S\}}dF+\frac{1}{2}\underset{1\times 36}{\{\Delta\varepsilon_y\}^T}\int\limits_F\underset{36\times 6}{[H]}^T\underset{6\times 6}{[h_\alpha]}\,\underset{6\times 24}{[H]}\,dF\underset{1\times 24}{\{\Delta\varepsilon_y\}}-\\ -\underset{1\times 36}{\{\Delta U_y^g\}^T}\,\underset{36\times 36}{[T]}^T\int\limits_F\underset{36\times 3}{[A]}^T\,\underset{3\times 1}{\{q\}}dF-\frac{1}{2}\underset{1\times 36}{\{\Delta U_y^g\}^T}\,\underset{36\times 36}{[T]}^T\int\limits_F\underset{36\times 3}{[A]}^T\underset{3\times 1}{\{\Delta q\}}dF+\\ +\underset{1\times 24}{\{\Delta S_y\}^T}\frac{1}{2}\int\limits_F\underset{24\times 6}{[H]}^T\,\underset{6\times 36}{[B]}\,dF\,\underset{36\times 36}{[T]}^T\underset{36\times 1}{\{\Delta U_y^g\}}-\underset{1\times 24}{\{\Delta S_y\}^T}\frac{1}{2}\int\limits_F\underset{24\times 6}{[H]}^T\underset{6\times 24}{[H]}\,dF\underset{24\times 1}{\{\Delta\varepsilon_y\}}.\end{gathered}\tag{3.8}$$

Minimising the functional (3.8) by nodal unknowns leads to the matrix equations

$$\frac{\partial \Pi_{LU}}{\partial\{\Delta\varepsilon_y\}^T} \equiv \underset{24\times24}{[a]}\,\underset{24\times1}{\{\Delta\varepsilon_y\}} - \underset{24\times24}{[d]}\,\underset{24\times1}{[\Delta S_y]} = 0; \tag{3.9}$$

$$\frac{\partial \Pi_{LU}}{\partial\{\Delta S_y\}^T} \equiv \underset{24\times36}{[b]}\,\underset{36\times1}{\{\Delta U_y\}} - \underset{24\times24}{[d]}^T\underset{24\times1}{[\Delta\varepsilon_y]} = 0; \tag{3.10}$$

$$\frac{\partial \Pi_{LU}}{\partial\{\Delta U_y^g\}^T} \equiv \underset{36\times24}{[b]}^T\,\underset{24\times1}{[\Delta S_y]} - \underset{36\times1}{\{f_{\Delta q}\}} + \underset{36\times1}{\{R\}} = 0, \tag{3.11}$$

where $\underset{24\times24}{[a]} = \int\limits_F \underset{24\times6}{[H]}^T \underset{6\times6}{[h_\alpha]}\,\underset{6\times24}{[H]}\,dF$; $\underset{24\times24}{[d]} = \frac{1}{2}\int\limits_F \underset{24\times6}{[H]}^T\,\underset{6\times24}{[H]}\,dF$; $\underset{24\times36}{[b]} = \frac{1}{2}\int\limits_F \underset{24\times6}{[H]}^T\,\underset{6\times36}{[B]}\,dF\,\underset{36\times36}{[T]}$; $\underset{36\times1}{\{f_{\Delta q}\}} = \underset{36\times36}{[T]}\int\limits_F \underset{36\times3}{[A]}^T\underset{3\times1}{\{\Delta q\}}dF$; $\underset{36\times1}{\{R\}} = -\underset{36\times36}{[T]}\int\limits_F \underset{36\times3}{[A]}^T\underset{3\times1}{\{q\}}dF + \underset{36\times36}{[T]}\int\limits_V \underset{6\times36}{[B]}\,\underset{36\times1}{\{S\}}dV$.

From the systems (3.9), (3.10) we obtain the relations

$$\underset{24\times1}{\{\Delta\varepsilon_y\}} = \underset{24\times24}{[d]}^{-1}\,\underset{24\times36}{[b]}\,\underset{36\times1}{\{\Delta U_y^g\}};\ \underset{24\times1}{\{\Delta S_y\}} = \underset{24\times24}{[d]}^{-1}\,\underset{24\times24}{[a]}\,\underset{24\times1}{\{\Delta\varepsilon_y\}}. \tag{3.12}$$

By considering (3.12), the stiffness matrix of the finite element is obtained from the system (3.11)

$$\underset{36\times36}{[K]}\,\underset{36\times1}{\{\Delta U_y^g\}} = \underset{36\times1}{\{f_{\Delta q}\}} - \underset{36\times1}{\{R\}}, \tag{3.13}$$

where $\underset{36\times36}{[K]} = \underset{36\times24}{[b]}^T\left[\underset{24\times24}{[d^T]^{-1}}\right]\underset{24\times24}{[a]}\,\underset{24\times24}{[d]}^{-1}\,\underset{24\times36}{[b]}$ — finite element stiffness matrix, which is used to form the shell stiffness matrix.

After determining the kinematic nodal unknowns of the shell, the deformation and force nodal unknowns are determined by (3.12).

4. Calculation example

As an example, the calculation of a shell with a medial surface in the form of a truncated ellipsoid of rotation loaded with internal pressure of intensity $q = 6$ MPa. Due to axial symmetry, the ellipsoid was modelled by a ribbon of discretisation elements oriented along the shell meridian. The left end of the shell was rigidly clamped, the right end was free of clamping (Fig. 1). The initial data had the following values: ellipsoid parameters $a = 1.3$ m; $b = 0.9$ m; thickness $h = 0.02$ m; axial coordinate varied in the range $0 \leqslant x \leqslant 1.2$ m. Mechanical characteristics of the shell material: duralumin alloy $E = 7.49\cdot10^4$ MPa; $\nu = 0.32$. The yield strength of the material is $\sigma_T = 200$ MPa. The deformation diagram was modelled by a two-link broken line with linear hardening defined by the dependence

$$\sigma_i = 200 + 18087(\varepsilon_i - 0,0023496). \tag{4.1}$$

The calculations were performed with control of the convergence of the computational process both by the number of sampling elements and by the number of loading steps. Tab. 1 shows the results of ellipsoidal shell calculation with the number of sampling elements equal to 200 and different numbers of loading steps. The table shows the values of normal stresses in the support and free ends of the shell on the inner σ^{in}, outer σ^{out} and midline σ^{midl} surfaces of the shell. Analyses of the tabular data allow us to conclude that the computational process is stable as the number of loading steps increases. Due to the unloaded right end of the ellipsoid, σ_{xx}^{midl} must be

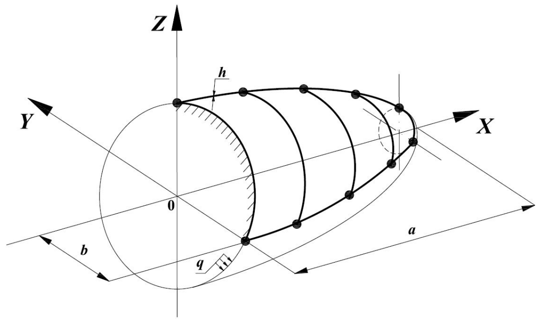

Fig. 1. Calculation diagram of an ellipsoidal shell

equal to zero. As Tab. 1 shows, the numerical values of σ_{xx}^{midl} are quite close to zero. The ring stresses σ_{tt}^{midl} at the free end of the ellipsoid can be calculated using the Laplace formula

$$\frac{\sigma_{xx}}{R_1} + \frac{\sigma_{tt}}{R_t} = \frac{q}{t}, \tag{4.2}$$

where $R_1,\ R_t$ are the radii of the principal curvatures.

Given that at the free end $\sigma_{xx} = 0$, the analytical value of σ_{tt} can be obtained from (4.2). $\sigma_{tt} = \frac{q}{t} R_t = \frac{6}{0.02} \cdot 0.6708 = 201.2$ MPa. Comparing the analytical value of σ_{tt}, presented in the rightmost column of Table 1, with the numerical value of σ_{tt}^{midl}, we can conclude that the calculation error $\delta = 3.38\%$ is within acceptable limits when performing engineering calculations.

Table 1. Numerical values of stresses depending on the number of loading steps

Point coordinates, x, m	σ, MPa	Number of loading steps				Analytical solution
		12	22	32	42	
0,00	σ_{xx}^{in}	322.6	321.1	319.8	320.1	—
	σ_{xx}^{out}	–230.4	–228.4	–227.2	–227.9	—
	σ_{xx}^{midl}	168.7	167.0	165.1	165.5	—
1,20	σ_{xx}^{in}	0.039	0.025	0.032	0.033	—
	σ_{xx}^{out}	0.041	0.030	0.036	0.036	—
	σ_{xx}^{midl}	0.036	0.023	0.030	0.030	0,00
	σ_{tt}^{in}	200.7	199.5	200.1	200.2	—
	σ_{tt}^{out}	189.5	188.3	188.9	1889	—
	σ_{tt}^{midl}	195.0	193.8	194.4	194.4	201.2

Conclusion

In the developed FEM algorithm in the three-field variant, when using bilinear approximations for deformation and force quantities to be sought, their coherence is ensured not only at the nodes of adjacent finite elements, but also along their boundaries. In addition, the developed algorithm can control the location of an internal point with coordinates $\varepsilon_i,\ \sigma_i$ on the deformation diagram, which opens up the possibility of finding unloading zones under complex loading of shell structures.

References

[1] Yu.Klochkov, A.Nikolaev, V.Pshenichkina, O.Vakhnina, M.Klochkov, Three-field fem for analysis of thin elastic shells, *Magazine of Civil Engineering*, **17**(2024), no. 3(127), 12710.

[2] Yu.V.Klochkov, V.A.Pshenichkina, A.P.Nikolaev, S.S.Marchenko, O.V.Vakhnina, M.Yu.Klochkov, Calculation of shells of revolution with the use of a mixed fem with a vector approximation procedure, *Journal of Machinery Manufacture and Reliability*, **53**(2024), no. 1, 10–21. DOI: 10.1134/S1052618824010059

[3] M.Cervera, M.Chiumenti, R.Codina, Mixed stabilized finite element methods in nonlinear solid mechanics: Part I: Formulation, *Comput. Meth. Appl. Mech. Eng.*, **199**(2010), no. 37-40, 2559–2570. DOI: 10.1016/j.cma.2010.04.006

[4] M.Cervera, M.Chiumenti, R.Codina, Mixed stabilized finite element methods in nonlinear solid mechanics: Part III: Compressible and incompressible plasticity, *Comput. Meth. Appl. Mech. Eng.*, **285**(2015), no. 1, 752–775. DOI: 10.1016/j.cma.2014.11.040

[5] N.A.Nodargi, P.Bisegna, A novel high-performance mixed membrane finite element for the analysis of inelastic structures, *Comput. Struct.*, **182**(2017), 337–353.
DOI: 10.1016/j.compstruc.2016.10.002

[6] F.S.Liguori, A.Madeo, G.Garcea, A mixed finite-element formulation for the elasto-plastic analysis of shell structures, *Materials Research Proceedings*, **26**(2023), 227–232.

[7] F.S.Liguori, A.Madeo, G.Garcea, A dual decomposition of the closest point projection in incremental elasto-plasticity using a mixed shell finite element, *International Journal for Numerical Methods in Eng.*, **123**(2022), 6243–6266.

[8] A.Bilotta, L.Leonetti, G.Garcea, An algorithm for incremental elastoplastic analysis using equality constrained sequential quadratic programming, *Comput. Struct.*, **102-103**(2012), 97–107.

[9] A.Bilotta, G.Garcea, L.Leonetti, A composite mixed finite element model for the elastoplastic analysis of 3D structural problems, *Finite Elcm. Anal. Des.*, **113**(2016), 43–53.
DOI: 10.1016/j.finel.2016.01.002

[10] L.A.M.Mendes, L.M.S.S.Castro, Hybrid-mixed stress finite element models in elastoplastic analysis, *Finite Elem. Anal. Des.*, **45**(2009), no. 12, 863–875.
DOI: 10.1016/j.finel.2009.06.021

[11] N.A.Nodargi, P.Bisegna, State update algorithm for isotropic elastoplasticity by incremental energy minimization, *Int. J. Numer. Methods Eng.*, **105**(2015), no. 3, 163–196.
DOI: 10.1002/nme.4966

[12] N.A.Nodargi, E.Artioli, F.Caselli, P.Bisegna, State update algorithm for associative elastic-plastic pressure-insensitive materials by incremental energy minimization, *Fracture and Structural Integrity*, **29**(2014), 111–127. DOI: 10.3221/IGF-ESIS.29.11

[13] A.Bilotta, L.Leonetti, G.Garcea, Three field finite elements for the elastoplastic analysis of 2D continua, *Finite Elem. Anal. Des.*, **47**(2011), no. 10, 1119–1130.
DOI: 10.1016/j.finel.2011.05.002

[14] A.Sh.Dzhabrailov, A.P.Nikolaev, Y.V.Klochkov, N.A.Gureeva, Accounting for displacement as a solid in the FEM algorithm for the calculation of shells of rotation, *Izvestia of the Russian Academy of Sciences. Mechanics of Solid State*, **6**(2023), 23–38 (in Russian).

[15] L.I.Sedov, Mechanics of Continuous Medium, Moscow, Nauka, Vol. 1, 1994 (in Russian).

Физически нелинейное деформирование оболочки при использовании трехпольного МКЭ

Михаил Ю. Клочков
Волгоградский государственный технический университет
Волгоград, Российская Федерация
Анатолий П. Николаев
Волгоградский государственный аграрный университет
Волгоград, Российская Федерация
Валерия А. Пшеничкина
Волгоградский государственный технический университет
Волгоград, Российская Федерация
Ольга В. Вахнина
Александр С. Андреев
Юрий В. Клочков
Волгоградский государственный аграрный университет
Волгоград, Российская Федерация

Аннотация. Разработана методика реализации при шаговом нагружении алгоритма определения напряженно-деформированного состояния (НДС) тонкой оболочки на основе метода конечных элементов (МКЭ) в трехпольной формулировке. В качестве конечного элемента принят четырехугольный фрагмент срединной поверхности тонкой оболочки. Узловыми неизвестными на шаге нагружения использованы: приращения кинематических величин (приращения перемещений и их производных); приращения деформационных величин (приращения деформаций и искривлений срединной поверхности); приращения силовых величин (приращения усилий и моментов). Аппроксимация кинематических величин осуществлялась с использованием бикубических функций формы на основе полиномов Эрмита третьей степени, а величин силовых и деформационных — с использованием билинейных функций. Для учета физической нелинейности материала оболочки использованы определяющие уравнения в двух вариантах: первый — определяющие уравнения теории пластического течения и второй — определяющие уравнения на основе предложенной гипотезы о пропорциональности компонент девиаторов приращений деформаций и приращений напряжений. Матрица жесткости конечного элемента сформирована на основе нелинейного функционала Лагранжа для шага нагружения, выражающего равенство возможных и действительных работ заданных нагрузок и внутренних усилий, с дополняющим условием равенства нулю действительной работы приращений внутренних усилий на разности приращений деформационных величин, определяемых геометрическими соотношениями и с использованием аппроксимирующих выражений. С использованием полученной матрицы жесткости конечного элемента дается пример расчета.

Ключевые слова: конечный элемент в трехпольной формулировке, физическая нелинейность материала, варианты определяющих уравнений, нелинейный функционал Лагранжа с условием.